JOURNAL OF MATERIALS SCIENCE 17 (1982) 1066–1078

Effects of anelastic deformation on high-temperature stress relaxation of polycrystalline MgO and Al_2O_3

YASURO IKUMA, RONALD S. GORDON
Department of Materials Science and Engineering, University of Utah, Salt Lake City, Utah 84112, USA

High-temperature (1160 to 1450° C) deformation of dense polycrystalline (10 to 90 μm) Al_2O_3 and MgO doped with Fe (up to 2.65 cation %) was studied by stress relaxation, dead-load creep and creep recovery. In some cases, all three deformation tests were conducted on a single specimen. A comparison of strain rate–stress data calculated from both stress relaxation and dead-load creep experiments revealed discrepancies in both the magnitude of the strain rates and the dependence between the strain rate and stress. These differences were attributed to the existence of anelastic deformation effects. The correction of stress relaxation data in the low stress regime for linear anelasticity led to strain rate–stress data in reasonably close agreement with results obtained from dead-load creep tests conducted in the viscous creep regime. Creep recovery experiments indicated that anelastic deformation in these ceramic materials was relatively insensitive to changes in temperature and grain size over the range of variables studied.

1. Introduction

An analysis for the calculation of plastic strain rates and stresses from stress relaxation measurements taken under conditions of four-point bending has been proposed by Shetty and Gordon [1]. In this analysis, the plastic deflection rate, $\dot{Y}$, of the specimen is calculated from

$$\dot{Y} = -C\frac{dP}{dt},$$

where C is the total elastic compliance of the system, including the specimen and the machine components such as the load cell and dP/dt is the rate of load relaxation. Shetty and Gordon assumed that stress relaxation is due entirely to the conversion of elastic strain to plastic strain. In the present paper, the validity of this assumption will be analysed by comparing strain rates calculated from stress relaxation and dead-load creep tests. It will be shown that anelastic effects have a significant effect on the interpretation of stress relaxation data. The effect of anelasticity on stress relaxation in metallic systems has been recognized by previous investigators [2–4]; however, the direct comparison of strain rates calculated from stress relaxation and dead-load creep tests is rare in deformation tests at high temperatures on ceramic materials [5].

2. Experimental procedure

Specimens tested in this study included dense polycrystalline MgO doped with 2.65 cation % Fe and polycrystalline Al_2O_3 doped with 1 to 2 cation % Fe, with grain sizes, G_S, between 10 and 90 μm. These materials and dopants were selected because extensive dead-load creep data were available [6, 7] in these systems for comparison with stress relaxation data. The methods used in the preparation of these specimens have been described elsewhere [6, 7]. Stress relaxation tests were performed in four-point bending using an apparatus described by Shetty and Gordon [1]. Creep recovery experiments were performed using a four-point dead-load creep apparatus, with a remote unloading system which is described elsewhere [8].

0022–2461/82/041066–13$04.06/0

In the stress relaxation tests, plastic strain rates and stresses were calculated from

$$\dot{\epsilon}_{max} = \frac{4h}{a^2}(\dot{Y}_C - \dot{Y}_L)$$
$$= \frac{4h}{a^2}[\dot{P}(t)(C_L - C_C) + \dot{Y}_{Ct}(t)], \quad (2)$$

where $\dot{\epsilon}_{max}$ is the maximum plastic strain rate in the outer fibre, $\dot{Y}_C$ is the plastic deflection rate at the centre of the beam, $\dot{Y}_L$ is the plastic deflection rate at the load points, h is the thickness of the beam, a is the distance between load points, $\dot{Y}_{Ct}$ (t) is the total centre-point deflection rate at any time t, $\dot{P}$ (t) is the corresponding rate of load change at time t, and C_C and C_L are the elastic centre-point and load-point compliances, respectively, and from

$$\sigma_{max} = \frac{Mh}{2I}\frac{2N'+1}{3N'}, \quad (3)$$

where

$$N' = \frac{d \log \dot{\epsilon}_{max}}{d \log M},$$

M is the bending moment in the inner span and I is the moment of inertia of the cross-section.

3. Results

3.1. Stress relaxation

Typical strain rate–stress data calculated from stress relaxation tests at 1350° C on polycrystalline MgO doped with iron are shown in Fig. 1. A series of creep tests have been conducted on similar specimens [6] and creep maps have been constructed [9] from steady-state dead-load creep data. The stress–strain rate characteristics predicted from the creep maps are indicated by the broken lines in Fig. 1. In both polycrystalline MgO and Al_2O_3, two deformation regimes were readily apparent. At low stresses, viscous (or diffusional) creep was dominant, while at higher stresses power-law or exponential creep mechanisms dominated. A comparison of the two sets of deformation data revealed several important differences. The quantitative agreement in the magnitude of the strain rates at a fixed stress between these two types of experiments was poor. The strain rates calculated from the stress–relaxation tests were higher than those measured in dead-load creep in the high stress regime. However, in the low stress regime the strain rates measured in dead-load creep were higher than

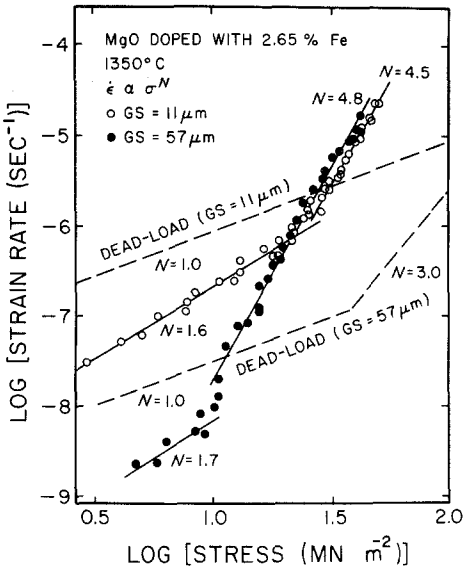

Figure 1 Strain rate–stress behaviour of polycrystalline MgO doped with 2.65 cation% Fe tested by stress relaxation and dead-load creep.

those calculated from stress relaxation data. Disagreement of this kind was observed in the high-temperature deformation of both polycrystalline MgO and Al_2O_3. In addition to differences in strain rates, discrepancies also existed in the observed dependencies between strain rate and stress. The stress exponents (i.e., N; $\dot{\epsilon} \propto \sigma^N$) in both the low and high stress regimes calculated from stress relaxation data were higher than those inferred from dead-load creep data. To determine if the foregoing differences in deformation characteristics were due to variabilities in the specimens used in the two types of tests, some specimens were first tested under conditions of dead-load creep and then stress relaxation tests were performed on the same specimens. The dead-load creep data were in agreement with the predictions of the creep maps; however, the strain rate–stress curves calculated from the stress relaxation data did not agree with the predictions of the maps. It was therefore concluded that the results shown in Fig. 1 were not due to different characteristics in the test specimens but to differences inherent in the dead-load creep and stress relaxation modes of deformation.

In metallic systems, the disagreement in strain rates calculated from dead-load and stress relaxation data has been observed [2]. As far as the authors are aware, the only comparison in a ceramic system of strain rates calculated from both dead-

TABLE I Creep recovery characteristics in polycrystalline MgO and Al_2O_3 doped with iron.

Base oxide	Impurity	Temperature (° C)	$\Delta\sigma$ (MN m^{-2})	τ^{-1} (min^{-1})				
				$G_S = 18\,\mu m$	$G_S = 89\,\mu m$	$G_S = 16\,\mu m$	$G_S = 26\,\mu m$	$G_S = 29\,\mu m$
MgO	2.65% Fe	1160	10	4.6×10^{-3}	-			
MgO	2.65% Fe	1350	10	4.0×10^{-3}	1.3×10^{-3}			
MgO	2.65% Fe	1350	2.5	-	1.1×10^{-3}			
MgO	2.65% Fe	1425	10	-	8.9×10^{-4}			
Al_2O_3	2 % Fe	1300	5.8			-	3.7×10^{-3}	-
Al_2O_3	2 % Fe	1450	5.8			2.2×10^{-3}	2.1×10^{-3}	6.3×10^{-3}

load creep and stress relaxation was made by Roberts [5] for the high-temperature deformation of polycrystalline UO_2. Roberts reported close agreement between data generated by the two techniques. However, the stress relaxation and dead-load creep experiments were not performed on the same specimens. The dead-load creep data were taken from experiments of Bohaboy *et al.* [10]. More importantly, the ranges of strain rates and stresses for the two types of deformation tests did not overlap each other. Based on the results of this study, it is believed that dead-load creep and stress relaxation experiments should be performed within the same or overlapping range of stress before any definite conclusions can be drawn*.

In all stress relaxation tests, the load–relaxation cycle had to be repeated more than about five times before reproducible strain rate–stress curves were obtained. Typical load relaxation cycles are shown in Fig. 2a for polycrystalline Al_2O_3 doped with 1 cation% Fe. After several loadings, the strain rate–stress curves were reproducible. Both transient effects [11] and local deformation at the load and support points (i.e., portions of the specimens which are in the vicinities of these regions might relax during the test) might be responsible for the observed decay in strain rate at a given stress with multiple loading. Hart and Solomon [11] reported a decay in strain rate with multiple loading which is similar to that shown in Fig. 2a. They attributed the decay to be a non-recoverable transient. It has been verified experimentally in this study that if a given loading cycle (e.g. the sixth in Fig. 2b) is followed by a subsequent loading cycle (i.e., the seventh) in which the maximum stress is significantly lower, the strain rate–stress curve becomes similar to that observed in a previous cycle (e.g., the third cycle in Fig. 2b). This reversible characteristic indicated that the transient behaviour of the material was responsible for the observed decay in strain rate, particularly in loading cycles after the initial one. Although Hart and Solomon [11] concluded that the transient was non-recoverable, the results of this study indicated that transient deformation was reversible. An examination of test specimens after the stress relaxation experiments indicated that some localized deformation occured in the vicinity of the load and support points. However, it is believed that the decay in strain rate which existed after the initial loading, was due to the recoverable transient. The decay in strain rate due to any local deformation, is likely to be present only in the initial loading cycle. The stress relaxation results reported in this paper, other than those shown in Fig. 2a and b, were obtained after the fifth loading cycle.

3.2. Creep recovery and transient creep

Typical creep recovery data at 1350 to 1450° C are shown in Fig. 3. Prior to the creep recovery test, creep specimens were loaded at stresses up to 10 MN m^{-2} which were normally within the limit of viscous creep for the range of grain size studied in polycrystalline MgO and Al_2O_3. A single exponential relaxation could not be used to describe the entire recovery process. The data points taken in the initial stages of creep recovery did not lie on the straight line which could be used to fit the later stages of recovery. The relaxation times, τ, representing the final stages of creep recovery are summarized in Table I. Over the range of variables studied, the relaxation time for creep recovery was insensitive to variations in temperature, stress or grain size. These experiments were performed on the selected (about 5) specimens which were also

*It is possible that in the case of UO_2 the anelastic contributions to deformation are very small. However, this possibility is most unlikely because Bohaboy *et al.* [10] observed extensive transient creep behaviour in their compression creep experiments.

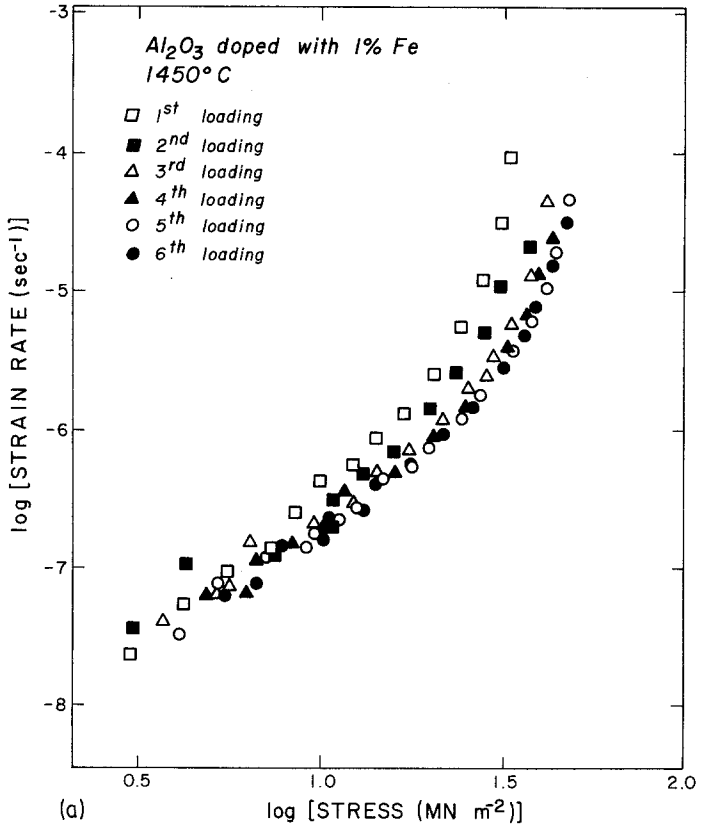

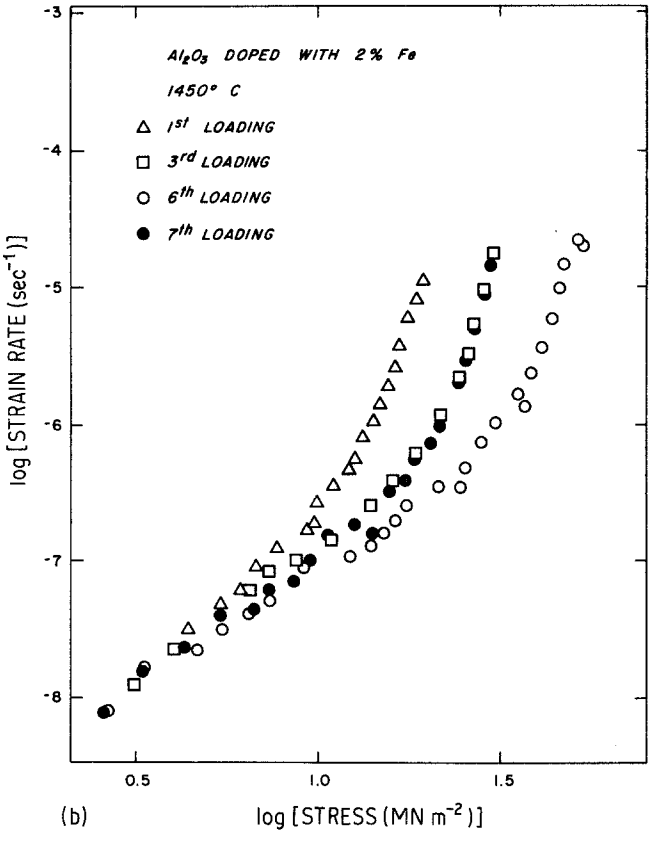

Figure 2 Effect of repeated loading on strain–stress behaviour obtained from stress relaxation tests on polycrystalline Al_2O_3 doped with iron.

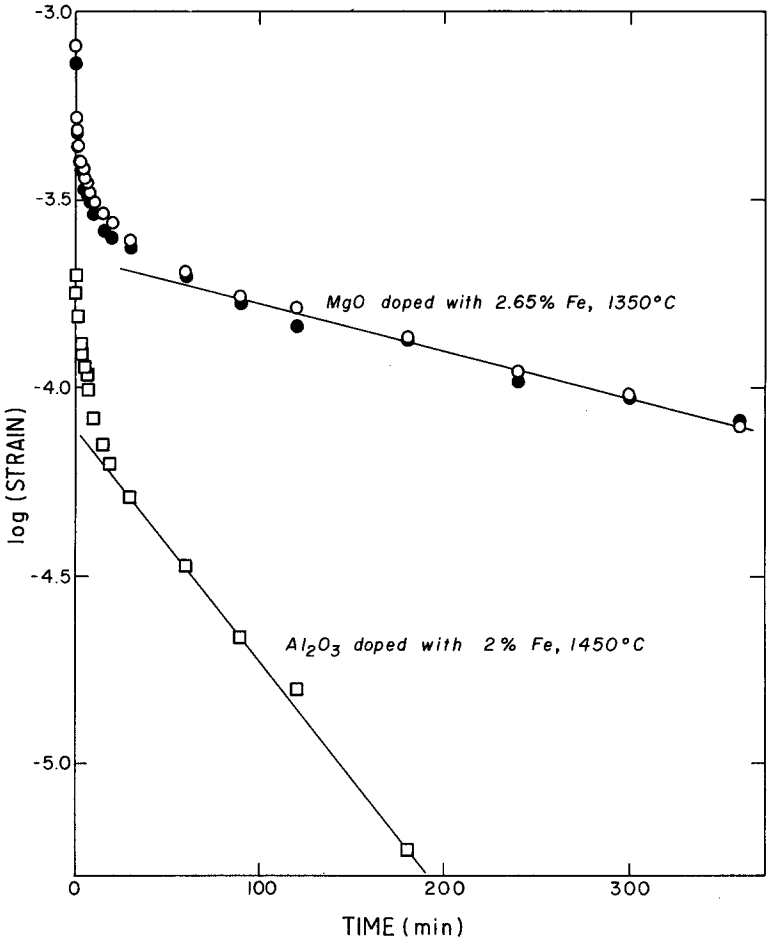

Figure 3 Creep recovery tests conducted on polycrystalline Al_2O_3 doped with 2 cation% Fe and polycrystalline MgO doped with 2.65 cation % Fe.

tested in stress relaxation. Consequently, a limited range of temperatures and grain sizes were studied. The primary objective of the recovery experiments was to generate material constants which were needed to evaluate the anelastic effects in stress relaxation.

The transient and recovered strains observed in typical dead-load creep and creep recovery tests are summarized in Table II. Dead-load creep was first measured and then creep recovery was examined. The loading–unloading cycle was repeated several times. The strains in Table II are listed in the order in which the experiments were performed. Except for the first loading cycle, the transient strain was recovered completely during loading. The effects of grain size, temperature and stress on the transient and recovered strains were not significant over the range of variables studied.

4. Discussions and analysis

At extended times in a stress relaxation test on a polycrystalline material which can deform by a diffusional (or viscous) creep mechanism, one might except stress relaxation to obey an equation of the form

$$\sigma = \sigma_0 \exp(-E_1 t/\eta_1), \qquad (4)$$

where E_1 is the elastic modulus, σ_0 is the initial stress and η_1 is the viscous (diffusional) creep viscosity ($= kTG_S^3/44\Omega_V D_{complex}$, where k is the Boltzmann's constant, T is the absolute temperature, G_S is the grain size, Ω_V is the molecular volume and $D_{complex}$ is the complex diffusivity). Accordingly, it should be possible to measure the term, E_1/η_1, from stress relaxation, compute η_1 knowing E_1, and compare the calculated viscosity with that computed from dead-load diffusional creep measurements (i.e., $\dot{\epsilon} = \sigma/\eta_1$). When this comparison was made for polycrystalline Al_2O_3 doped with 1 % Fe, reasonably good agreement was achieved between η_1 (2.4×10^{13} N sec m^{-2}) computed from stress relaxation data taken at long times and η_1 (2.2×10^{13} N sec m^{-2}) calculated from diffusional creep data (i.e., $D_{complex} = f(D^1_{Al}$

TABLE II Transient and recovered strain observed in dead-load creep and creep recovery

Base oxide	Dopant	G_S (μm)	T (° C)	$\Delta\sigma$ (MN m^{-2})	Transient strain (creep) ($\times 10^{-4}$)	Recovered strain (creep recovery) ($\times 10^{-4}$)
Al_2O_3	2 % Fe	16	1450	5.6	6.3	2.1
Al_2O_3	2 % Fe	16	1450	5.6	2.8	2.9
Al_2O_3	2 % Fe	16	1450	5.6	2.7	3.1
Al_2O_3	2 % Fe	26	1450	6.0	4.3	1.9
Al_2O_3	2 % Fe	26	1450	6.0	1.7	2.3
Al_2O_3	2 % Fe	26	1300	6.0	1.5	1.4
Al_2O_3	2 % Fe	26	1300	6.0	1.2	1.1
Al_2O_3	2 % Fe	29	1450	5.8	3.8	2.6
Al_2O_3	2 % Fe	29	1450	5.8	2.7	-
MgO	2.65 % Fe	18	1350	10.0	6.1	4.6
MgO	2.65 % Fe	18	1350	10.0	3.9	3.6
MgO	2.65 % Fe	18	1160	10.0	2.8	3.2
MgO	2.65 % Fe	89	1350	2.5	4.8	4.2
MgO	2.65 % Fe	89	1350	2.5	3.2	3.4
MgO	2.65 % Fe	89	1350	10.0	-	6.4
MgO	2.65 % Fe	89	1350	10.0	4.1	6.0
MgO	2.65 % Fe	89	1350	2.5	-	3.9
MgO	2.65 % Fe	89	1425	10.0	4.2	6.3

and $\delta_{Al}D^b_{Al}$), where D^l_{Al} is the aluminium lattice diffusivity and D^b_{Al} is the aluminium grain-boundary diffusivity and δ_{Al} is the effective width for aluminium grain-boundary diffusion). Even with this agreement, the correspondence between the actual creep rates calculated from both stress relaxation and dead-load creep data was poor.

Two principal assumptions were made in the calculation of strain rates from stress relaxation data: (1) the testing machine and loading system had a high stiffness and (2) no anelastic deformation contributions were present. The effect of machine relaxation, including that of the loading system, can be determined from a stress relaxation test conducted on a "stiff" specimen. An undoped alumina specimen with a thickenes of about 14 mm (a typical thickness was about 1.4 to 1.5 mm) was tested by stress relaxation and the deflection rate–load behaviour was measured. In specimens, such as Al_2O_3 doped with 1 to 2% Fe and MgO doped with 0.53 to 2.65% Fe, the deflection rate of the specimen was about two orders of magnitude higher than the deflection rate of the "stiff" specimen. Therefore, it was reasonable to conclude that the stress relaxation of machine components and the loading system did not cause the discrepancies observed in strain rates which were computed from both dead-load creep and stress relaxation tests.

In the stress relaxation analysis of Shetty and Gordon, the following assumption for total strain was made:

$$\epsilon_{Total} = \epsilon_{Elastic} + \epsilon_{Plastic}. \quad (5)$$

For stress relaxation at constant total strain,

$$\dot{\epsilon}_{Total} = 0 = \dot{\epsilon}_{Elastic} + \dot{\epsilon}_{Plastic} \quad (6)$$

and

$$\dot{\epsilon}_{Plastic} = -\dot{\epsilon}_{Elastic} = -\frac{\dot{\sigma}}{E}. \quad (7)$$

That is, in stress relaxation, the elastic (instantaneous recoverable) strain is converted into plastic strain. If diffusional (viscous) creep represents the plastic strain, then we have the classical Maxwell body corresponding to a spring and dash-pot in series. A generalized Maxwell body including viscous and elastic elements should have the following creep characteristics:

(a) On the application of the load, elastic deformation takes place instantly, followed by steady-state creep. No transient creep should be observed.

(b) When the load is removed after the creep test, the elastic strain will be recovered instantly. However there will be no time-delayed strain recovery.

Careful examination of the dead-load creep characteristics of polycrystalline MgO and Al_2O_3 revealed, however, the presence of significant transient creep at the beginning of the test (about

10 h) and, more importantly, the occurence of significant recovery (time-delayed recoverable strain) when the stress was removed. These observations were consistent with the presence of an anelastic contribution which can be approximately represented by a Maxwell–Voigt (or Kelvin) deformation model [2]. In this model, the following behaviour is predicted for creep under dead-load conditions.

(1) After instantaneous elastic deformation, transient deformation which is recoverable should occur prior to the on-set of steady-state deformation, i.e.,

$$\epsilon = a + bt + c(1 - e^{-t/\tau}), \tag{8}$$

where a, b, c and τ are constants.

(2) When the specimen is unloaded during dead-load creep, the anelastic Voigt (or Kelvin) element will lead to creep recovery.

$$\epsilon = C_1 e^{-t/\tau} + d, \tag{9}$$

where C_1 and d are constants.

(3) The stress relaxation curve will have two exponential terms,

$$P = C_1 e^{-t/\tau_1} + C_2 e^{-t/\tau_2}, \tag{10}$$

where C_2, τ_1 and τ_2 are constants.

These properties suggest that the Maxwell–Voigt body is a better representation of the deformation characteristics encountered in this study than the simple Maxwell body. According to the Maxwell–Voigt deformation model

$$\epsilon_{\text{Total}} = \epsilon_{\text{Elastic}} + \epsilon_{\text{Plastic}} + \epsilon_{\text{Anelastic}}. \tag{11}$$

For stress relaxation,

$$\dot{\epsilon}_{\text{Total}} = 0 = \dot{\epsilon}_{\text{Elastic}} + \dot{\epsilon}_{\text{Plastic}} + \dot{\epsilon}_{\text{Anelastic}} \tag{12}$$

and

$$\dot{\epsilon}_{\text{Plastic}} = -\frac{\dot{\sigma}}{E} - \dot{\epsilon}_{\text{Anelastic}}. \tag{13}$$

In the stress relaxation analysis of Shetty and Gordon [1], $\dot{\epsilon}_{\text{Anelastic}}$ was assumed to be small or zero. This can only be strictly valid in the absence of transient creep and recovery effects.

In Equation 13, the first term is positive since $\dot{\sigma} < 0$. At short times in a stress relaxation test, $\dot{\epsilon}_{\text{Anelastic}} (= \sigma/\eta_2) > 0$ (assuming a Voigt element, $\epsilon = \sigma/E_2\,(1 - \exp - E_2 t/\eta_2)$) and $\dot{\epsilon}_{\text{plastic}}$ will be overestimated, when $\dot{\epsilon}_{\text{Anelastic}}$ is assumed to be zero. At long times, $\dot{\epsilon}_{\text{Anelastic}} (= \dot{\sigma}/E_2) < 0$ and $\dot{\epsilon}_{\text{Plastic}}$ will be underestimated when $\dot{\epsilon}_{\text{Anelastic}}$ is ignored. These effects were in accord with the general experimental observations (e.g. Fig. 1).

In a dead-load creep test, the effects of anelasticity are also present, but only during initial transient creep (see Equation 8). Once steady-state creep has been achieved, all anelastic effects are completely relaxed. Only the Maxwell element is present in the steady-state creep regime.

Thus, it appears that anelastic deformation effects were responsible for the lack of direct correspondence between dead-load creep rates and those calculated from stress relaxation measurements assuming "Maxwellian" behaviour. The initial objective of the stress relaxation study was to construct creep deformation maps in the high stress regime where dead-load creep testing is difficult because of excessive deformation strains. However, stress relaxation tests may not be suitable for this purpose unless the anelastic contributions to deformation can either be suppressed or taken into account in the analysis of the data.

The problem is the extent to which anelasticity affects the stress relaxation test. This is difficult to assess because the materials investigated in this study could not be represented simply by a viscoelastic Maxwell–Voigt body. However, the effect of anelasticity on viscous (diffusional) deformation can be shown by comparing the stress relaxation curves typical of two simplified models: i.e., viscoelastic Maxwell–Voigt and Maxwell bodies. The Maxwell–Voigt element is shown in Fig. 4. In this model, it is assumed that the spring obeys Hooke's law and that the dash-pot represents the viscous element. A mathematical expression

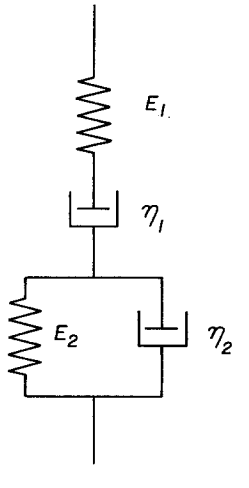

Figure 4 Maxwell–Voigt (or Kelvin) deformation model.

TABLE III Material characteristics for the Maxwell–Voigt deformation contribution in polycrystalline Al_2O_3 and MgO

Element	Source	2% Fe–Al_2O_3 (1450° C)	2.65% Fe–MgO (1350° C)
E_1	[12, 13]	1.0×10^{11} N m^{-2}	2.15×10^{11} N m^{-2}
E_2*	Assumed	4.0×10^{11} N m^{-2}	8.60×10^{11} N m^{-2}
η_1	Dead-load creep	4.01×10^{13} N sec m^{-2}	3.10×10^{14} N sec m^{-2}
η_2	Creep recovery	4.14×10^{14} N sec m^{-2}	4.44×10^{15} N sec m^{-2}

*$E_2 = 4E_1$

for the stress relaxation behaviour of this body is given by (see the Appendix):

$$\sigma(t) = \frac{\sigma_0 \eta_1}{E_1}\left[\left(a-b-\frac{E_1}{\eta_2}\right)e^{-(a-b)t} + \left(a+b-\frac{E_2}{\eta_2}\right)e^{-(a+b)t}\right] \quad (14)$$

where

$$a = 1/2\left(\frac{E_1}{\eta_1}+\frac{E_1}{\eta_2}+\frac{E_2}{\eta_2}\right), \quad (15)$$

$$b = \left(a^2 - \frac{E_1 E_2}{\eta_1 \eta_2}\right)^{1/2} \quad (16)$$

and σ_0 is the initial stress. In the limit of $\eta_2 = \infty$, which corresponds to an absence of anelasticity (i.e., no Voigt element), Equation 14 simplifies to

$$\sigma = \sigma_0 e^{-\frac{E_1}{\eta_1}t}, \quad (17)$$

which is the expression expected for the Maxwell body. For the case of polycrystalline Al_2O_3 and MgO doped with Fe, estimates have been made for the E and η values of the Maxwell–Voigt body using data taken from dead-load creep and creep recovery experiments. The Young's moduli of polycrystalline Al_2O_3 and MgO at high temperature (1350 to 1450° C) were obtained from values published in the literature [12, 13]. The value of E_2 was arbitrarily set because there was no convenient way to estimate it. If E_1 was assumed simply to be equal to E_2, a stress relaxation curve was obtained that approached zero stress from negative values when t is large. To avoid this problem, E_2 was arbitrarily set at $4E_1$. The steady-state dead-load creep rate is equal to σ/η_1. Knowing the value of σ, the value of η_1 was estimated. The values of η_2 were obtained from the final slopes ($= -E_2/\eta_2$) of creep recovery curves in Fig. 3. These estimates are summarized in Table III.

Using Equation 14 and 17, a series of theoretical stress relaxation curves was generated. The analysis of Shetty and Gordon [1] (using Equations 2 and 3) was conducted on these calculated stress relaxation curves. The resulting strain rate against stress data are plotted in Fig. 5 for the deformation of polycrystalline Al_2O_3 doped with iron. Even though the Maxwell model represents viscous (or linear) behaviour ($N = 1$), the analysis of stress relaxation on the same material, when a Voigt element is introduced, led to the existence of slightly non-viscous (or non-linear) behaviour ($N \sim 1.3$). Also, in the low stress regime, the stress relaxation data obtained from the Maxwell–Voigt model led to lower creep rates than those inferred from the Maxwell model. These results were consistent with the experimental observations (see Fig. 1). Of course, the disagreement between the strain-rate predictions of these two models was not as large as that observed experimentally. For reasons of mathematical simplicity, only viscous (or linear) behaviour was assumed. If non-linear behaviour is taken into account*, the disagreement between creep rates calculated from the stress relaxation and dead-load creep data should be even larger.

In order to determine the effect of anelasticity on the stress relaxation tests, the following calculations were made. For a given initial maximum stress, σ_0, the stresses $\sigma_M(t)$ and $\sigma_{M-V}(t)$ were calculated as a function of time using Equations 17 and 14, respectively, and the data in Table III. The load, $P_M(t)$, corrected for anelastic deformation, can be given by

$$P_M(t) = \frac{\sigma_M(t)}{\sigma_{M-V}(t)} \cdot P(t), \quad (18)$$

where $P(t)$ is the actual load measured experimen-

*Another dash-pot is added in series which has non-linear deformation characteristics.

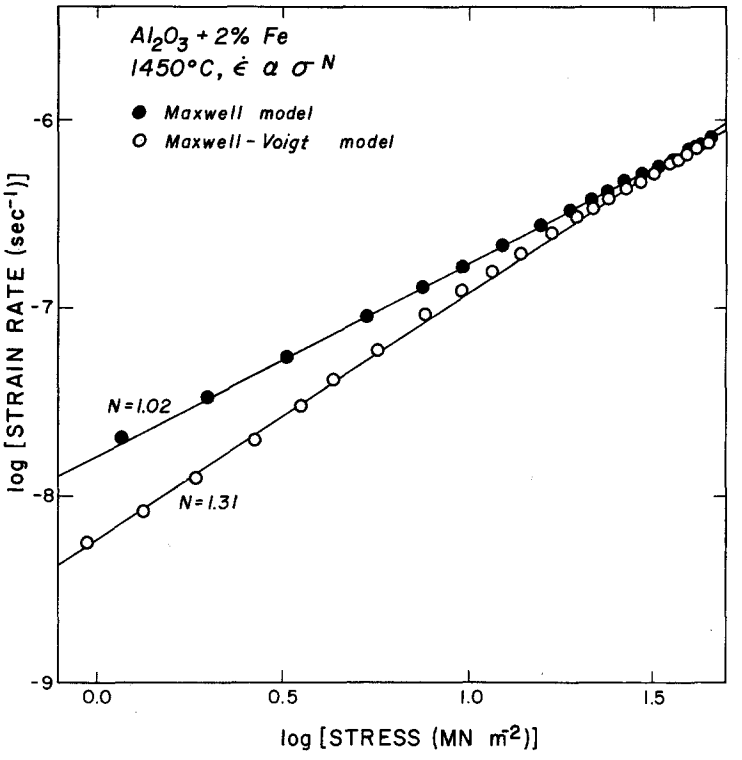

Figure 5 Strain rate–stress behaviour of model materials which are represented by viscoelastic Maxwell–Voigt (or Kelvin) and Maxwell elements.

tally, $\sigma_M(t)$ is the theoretical time dependent Maxwell stress and $\sigma_{M-V}(t)$ is the theoretical time dependent Maxwell–Voigt stress. $P_M(t)$ data, which were corrected at least for linear anelasticity, were analysed using Equations 2 and 3. The analysis of the two stress relaxation curves, with and without the linear anelastic correction, led to the results shown in Figs 6 and 7. In both cases, the stress exponent in the low-stress regime decreased from a high value (~ 2) to the expected viscous value of 1. The absolute strain rate in the low-stress regime either increased to the value predicted from dead-load creep, as in the case of MgO, or approached the dead-load creep value, as in the case of Al_2O_3. The differences in the absolute quantitative agreement in the tests on these two materials are probably due to the uncertainties involved in estimating the material parameters (E, η) in the Voigt and Maxwell elements. On the other hand, the strain rates in the high-stress regime were not affected by this analysis. The disagreement in strain rates at high stresses, which existed after the linear anelastic correction was made, was probably due to two factors. First, creep recovery could not be represented by a single exponent term (Fig. 3). A short time relaxation occurred in creep recovery which had a large effect on the strain rate calculated from the data in the high-stress regime of the stress relaxation test. Second, only viscous (or linear) behaviour was assumed to be operative in plastic deformation. Power-law (or non-viscous) creep, which was neglected in the Maxwell–Voigt model for mathematical simplicity, has a large effect on the strain rate in the high-stress regime. No correction was made for the effect of power-law (or non-viscous) creep deformation.

The data shown in Figs 6 and 7 indicated that anelasticity was the principal cause of the disagreement in strain rates inferred from stress relaxation and dead-load creep data. Difficulties exist in the analysis of anelastic deformation because the effect of the anelastic element on stress relaxation is not additive (compare with Equation 14) and because the linear Maxwell–Voigt body is not a completely adequate representation of the materials which were studied. The effect of anelastic deformation on the stress relaxation test is not simple. Although it has been common practice in the literature [3, 4, 14] to assume that anelasticity is linear in nature, the disagreement at high stresses in strain rates calculated from dead-load creep tests and anelastically corrected stress relaxation tests indicated that there should be another non-linear, anelastic element to describe the deformation properties

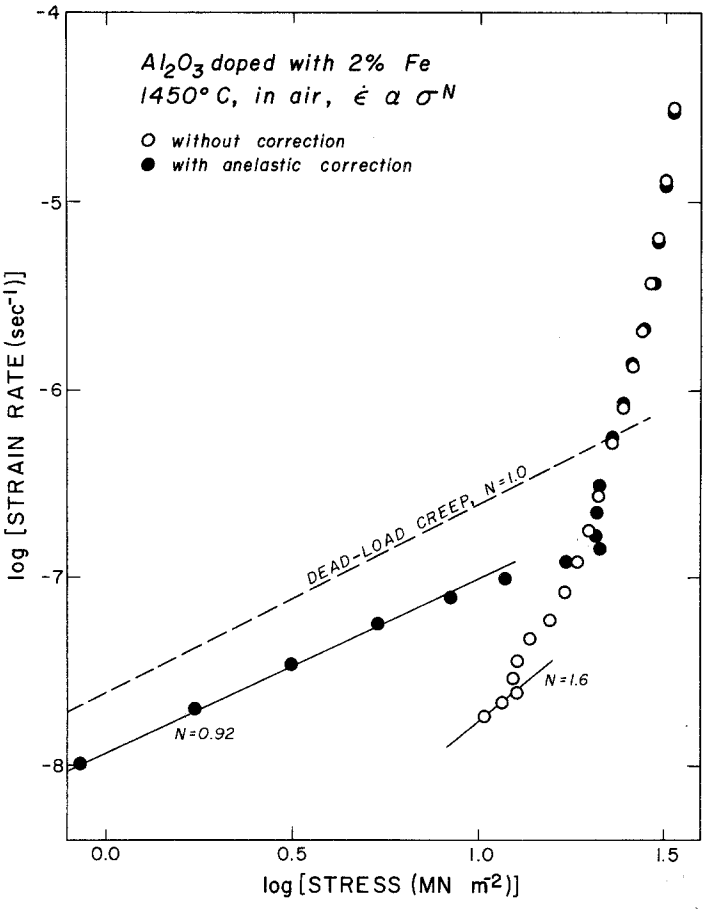

Figure 6 Effect of linear anelasticity on the strain rate–stress behaviour of polycrystalline Al_2O_3 doped with 2 cation % Fe.

in the high-stress regime. In terms of the simplified model, shown in Fig. 4, dash-pots which have non-linear characteristics should possibly be included in both the Voigt and Maxwell deformation elements. Unfortunately, the differential equations representing these models are non-linear and solutions must be obtained numerically. The reversible transient behaviour shown in Fig. 2b is probably due to the existence of a non-linear anelastic deformation element. It cannot be accounted for simply by the introduction of a permanent non-viscous (or power-law) deformation element.

The non-viscous (or power-law) strain rate-stress exponents obtained from dead-load creep tests were 2.5 to 5 and 2.5 to 3.5, for polycrystalline Al_2O_3 [7, 15, 16] and MgO [17–19], respectively. They were smaller than the stress exponents, of approximately 7 and 4.5, which were inferred from the stress relaxation data taken in this study. In view of the foregoing analysis, it was tentatively concluded that the higher stress exponents inferred from the stress relaxation tests were due, in part, to the effects of non-linear anelasticity.

A micromechanical discussion of anelasticity in metals has been given by Hart [3]. When dislocations are held up at obstacles and form pile-ups, a back stress will be exerted on dislocation gliding. Anelastic recovery could be due to the motion of dislocations which are held up by obstacles during loading. To a first approximation, the number and mobility of these dislocations could be relatively insensitive to changes in temperature, leading to athermal recovery effects. Stress redistribution controlled by diffusion [20] probably does not account for the observed anelastic behaviour because the activation energies for the diffusion of host ions in Al_2O_3 and MgO are very high (60 to 150 kcal mol^{-1}) [21–25]. Another possible cause of elasticity might be a diffusional redistribution of impurities caused by stress changes. Again the recovery process should be strongly temperature dependent. The activation energy for the diffusion of Fe^{2+} in MgO [26] is reported to be 42 kcal mol^{-1}, which gives a factor

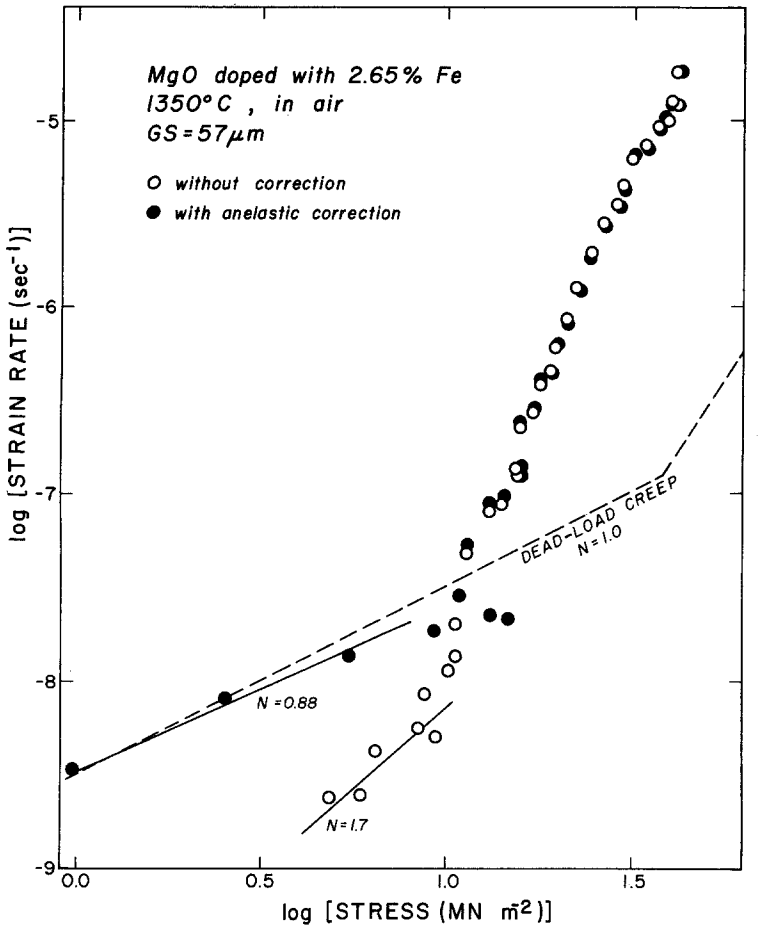

Figure 7 Effect of linear anelasticity on the strain rate–stress behaviour of polycrystalline MgO doped with 2.65 cation % Fe.

of about 6 change in the recovery relaxation time when the temperature is increased from 1160° C to 1350° C. Within the experimental accuracy (compare with Table I) of the recovery measurements, differences of this order are difficult to detect. Also, internal friction measurements [27] in single-crystal MgO have suggested that the peak height is proportional to the impurity (Cr and Fe) content and an activation energy of 49 kcal mol^{-1} (peak shift) was observed. The activation energy for the diffusion of Fe in Al_2O_3 is not known. Internal friction measurements [28] in polycrystalline Al_2O_3 led to an activation energy of approximately 50 kcal mol^{-1}, which is thought to be caused by viscous-phase stress relaxation at grain boundaries (Zener's theory*). The relatively low activation energy inferred from internal friction measurements on Al_2O_3 suggested that Zener's mechanism might be responsible for the anelastic effects observed in this study. Systematic and more extensive studies of high-temperature anelasticity are needed before any definite conclusions can be drawn for the deformation of polycrystalline Al_2O_3 and MgO. However, the preliminary data which are available suggest that anelastic deformation in these polycrystalline materials is athermal or weakly dependent on temperature.

5. Conclusions

The strain rates for the high-temperature deformation of iron-doped, polycrystalline Al_2O_3 and MgO which were calculated from both dead-load creep data and stress relaxation data were not in good agreement. The discrepancies were believed to be due to anelastic deformation effects. It is

*Zener [29] suggested that it is not necessary for any portion of material to be amorphous in order for the grain boundaries to behave in a viscous manner. It is necessary to assume only that the resistance to slipping of one grain over an adjacent grain obeys the laws commonly associated with amorphous materials rather than the laws associated with crystalline materials.

concluded that errors will be encountered in the analysis of stress relaxation, if it is assumed that the elastic strain is converted into only plastic strain and no anelastic contribution to deformation is considered. In dead-load creep tests, the contribution of anelasticity can be minimized because steady-state creep was observed, indicating that the anelastic deformation elements are completely relaxed. The method of strain-rate calculation proposed by Shetty and Gordon [1] for stress relaxation under conditions of four-point bending can only be used to calculate plastic strain rates provided that there is no anelastic contribution to deformation. Unless the contribution of anelasticity can be eliminated, or quantitatively taken into account, the stress relaxation test can not be used to construct creep maps together with data obtained from dead-load creep tests.

The effect of anelasticity on the stress relaxation test was demonstrated by making use of model materials which exhibit viscoelastic Maxwell and Maxwell–Voigt deformation characteristics. Even though a "Maxwellian" body shows viscous (or linear) creep behaviour ($N = 1$), the same material, when a Voigt element is introduced, deforms with slightly non-viscous (or non-linear) characteristics under conditions of stress relaxation. It was shown that by assuming linear anelasticity, the creep rates in the low-stress regime calculated from stress relaxation tests could be corrected to values which agreed with data obtained from dead-load creep. It is proposed that the discrepancies which existed in the high stress regime, after the corrections for linear anelasticity were made, will be removed only if another non-linear anelastic deformation element is taken into account.

Acknowledgement

The Department of Energy under Contract number EY-76-S-02-1591 is acknowledged for their support of this work.

Appendix: Analysis of stress relaxation in a Maxwell–Voigt (or Kelvin) deformation model

For a Maxwell deformation model, the appropriate differential equation is

$$\frac{1}{E_1}\frac{d\sigma}{dt}+\frac{1}{\eta_1}\sigma=\frac{d\epsilon}{dt}=0. \tag{A1}$$

Solving this equation and evaluating the constants using the appropriate initial boundary condition (i.e., at $t = 0, \sigma = 0$) gives

$$\sigma = \sigma_0 e^{-\frac{E_1}{\eta_1}t}. \tag{A2}$$

To find a solution for a stress relaxation test conducted on a Maxwell–Voigt body, let us assume for mathematical simplicity that the dash-pots in both the Maxwell and Voigt elements are viscous (or linear). Then, for the Maxwell–Voigt model shown in Fig. 4, the equations of stress and strain are given by

$$\sigma = E_2\epsilon_{an}+\eta_2\frac{d\epsilon_{an}}{dt} \tag{A3}$$

and

$$\frac{d\epsilon}{dt}=\frac{1}{E_1}\frac{d\sigma}{dt}+\frac{1}{\eta_1}\sigma+\frac{d\epsilon_{an}}{dt}, \tag{A4}$$

where ϵ_{an} is the strain for the Voigt element. The boundary conditions are

$$\text{At } t = 0,\ \sigma = \sigma_0; \tag{A5}$$

$$\text{At } t \geqslant 0,\ \epsilon = \text{constant}; \tag{A6}$$

$$\text{At } t = \infty.\ \sigma = 0; \text{and} \tag{A7}$$

$$\text{If } \eta_2 = \infty, \sigma = e^{-\frac{E_1}{\eta_1}t}. \tag{A8}$$

Condition A6 gives $d\epsilon/dt = 0$ and Equation A4 becomes

$$\frac{1}{E_1}\frac{d\sigma}{dt}+\frac{1}{\eta_1}\sigma+\frac{d\epsilon_{an}}{dt}=0. \tag{A9}$$

The solution to Equation A3 is

$$\epsilon_{an} = e^{-\frac{E_1}{\eta_2}t}\left[\frac{1}{\eta_2}\int e^{\frac{E_1}{\eta_2}t}\sigma\,dt+C_1\right]. \tag{A10}$$

Substituting ϵ_{an} into Equation A9 gives

$$\frac{E_2}{\eta_2}e^{\frac{-E_1}{\eta_2}t}\left[\frac{1}{\eta_2}\int e^{\frac{E_2}{\eta_2}t}\sigma\,dt+C_1\right]-\sigma\left(\frac{1}{\eta_1}+\frac{1}{\eta_2}\right) = \frac{1}{E_1}\frac{d\sigma}{dt}. \tag{A11}$$

Equation A11 can be solved by letting

$$Y(t) = e^{\frac{E_2}{\eta_2}t}\sigma(t)\,dt. \tag{A12}$$

and the solution is

$$\sigma(t) = \left(\frac{E_2}{\eta_2}-a+b\right)C_2e^{-(a-b)t} + \left(\frac{E_2}{\eta_2}-a-b\right)C_3e^{-(a+b)t}, \tag{A13}$$

where
$$a = 1/2\left(\frac{E_1}{\eta_2} + \frac{E_1}{\eta_2} + \frac{E_2}{\eta_2}\right) \quad \text{(A14)}$$

and
$$b = \left(a^2 - \frac{E_1 E_2}{\eta_1 \eta_2}\right)^{1/2}. \quad \text{(A15)}$$

C_2 and C_3 are constants to be evaluated. From Conditions A5 to A8 we can write
$$\sigma(t) = \frac{\sigma_0 \eta_1}{E_1}\left[\left(a - b - \frac{E_1}{\eta_2}\right)e^{-(a-b)t} + \left(a + b - \frac{E_2}{\eta_2}\right)e^{-(a+b)t}\right]. \quad \text{(A16)}$$

Freudenthal [2] combined Equations A3 and A4 and obtained a solution by a Laplace transformation assuming a step function for strain. The solution* is
$$\sigma(t) = \frac{\sigma_0}{2b}\left[\left(-a + b + \frac{E_2}{\eta_2}\right)e^{-(a-b)t} + \left(a + b - \frac{E_2}{\eta_2}\right)e^{-(a+b)t}\right]. \quad \text{(A17)}$$

The difference between the two solutions (Equations A16 and A17) arises from their different boundary conditions. The solution derived in this study is consistent with the behaviour of a Maxwell–Voigt element when the strain is held constant with the boundary conditions given by Equations A5 to A8. However, the solution obtained by Freudenthal describes the behaviour of the model when a step strain is applied. In this case, the solution corresponds to an instantaneous change in strain (delta-function for $\dot{\epsilon}$). If the strain was changed gradually with a finite strain rate which will be the case for actual experiments), the solution will change slightly. The differences in the constants in these two solutions reflect the different boundary conditions. However, the two solutions are basically the same. The more important point is that the stress calculated for the Maxwell model (Equation A2) has only one exponential term. When a Voigt element is introduced, the stress must be expressed by two exponential terms (Equations A16 and A17).

References

1. D. K. SHETTY and R. S. GORDON, *J. Mater. Sci.* **14** (1979) 2163.
2. A. M. FREUDENTHAL, *ASTM Proc.* **60** (1960) 986.
3. E. W. HART, *Nucl. Eng. Design* **46** (1978) 179.
4. *Idem*, in "Stress Relaxation Testing", ASTM STP 676, edited by A. Fox, (American Society for the Testing of Metals, Philadelphia, 1979) p. 5.
5. J. T. A. ROBERTS, *Acta Metal.* **22** (1974) 873.
6. R. T. TREMPER, R. A. GIDDINGS, J. D. HODGE, and R. S. GORDON, *J. Amer. Ceram. Soc.* **57** (1974) 421.
7. P. A. LESSING and R. S. GORDON, *J. Mater. Sci.* **12** (1977) 2291.
8. Y. IKUMA, Ph. D. Thesis, University of Utah (1980).
9. J. D. HODGE, P. A. LESSING and R. S. GORDON, *J. Mater. Sci.* **12** (1977) 1598.
10. P. E. BOHABOY, R. R. ASAMOTO and A. E. CONTI, GEAP-10054 (1969).
11. E. W. HART and H. D. SOLOMON, *Acta Metal.* **21** (1973) 295.
12. W. H. GITZEN, "Alumina as a Ceramic Material" (American Ceramic Society, Columbus, Ohio, 1970) p. 53.
13. D. H. CHUNG and W. G. LAWRENCE, *J. Amer. Ceram. Soc.* **47** (1964) 448.
14. G. J. LLOYD and R. J. McELROY, *Acta Metal.* **22** (1974) 339.
15. W. R. CANNON and O. D. SHERBY, *J. Amer. Ceram. Soc.* **56** (1973) 157.
16. S. I. WARSHAW and F. H. NORTON, *ibid.* **45** (1962) 479.
17. J. H. HENSLER and G. V. CULLEN, *ibid.* **51** (1968) 557.
18. G. R. TERWILLINGER, H. K. BOWEN and R. S. GORDON, *ibid.* **53** (1970) 241.
19. T. G. LANGDON and J. A. PASK, *Acta Metal.* **18** (1970) 505.
20. R. S. GORDON and G. R. TERWILLINGER, *J. Amer. Ceram. Soc.* **55** (1972) 450.
21. Y. OISHI and W. D. KINGERY, *J. Chem. Phys.* **32** (1960) 480.
22. A. E. PALADINO and W. D. KINGERY, *ibid.* **37** (1962) 957.
23. Y. OISHI and W. D. KINGERY, *ibid.* **33** (1960) 905.
24. R. LINDER and G. D. PARFITT, *ibid.* **26** (1957) 182.
25. B. C. HARDING and D. M. PRICE, *Phil. Mag.* **26** (1972) 253.
26. B. J. WUENSCH and T. VASILOS, *J. Chem. Phys.* **36** (1962) 2917.
27. P. D. SOUTHGATE, *J. Phys. Chem. Sol.* **27** (1966) 1263.
28. J. E. TURNBAUGH and F. H. NORTON, *J. Amer. Ceram Soc.* **51** (1968) 344.
29. C. ZENER, "Elasticity and Anelasticity of Metals" (University of Chicago Press, Chicago, 1948) pp. 147–159.
30. W. N. FINDLEY, J. S. LAI and K. ONARAN, "Creep and Relaxation of Nonlinear Viscoelastic Materials", (North-Holland Publishing, Amsterdam, New York and Oxford, 1976).

Received 19 January
and accepted 15 September 1981

*Findely *et al.* [30] also obtained the solution in a similar fashion.